



Half-metallic surface states and topological superconductivity in NaCoO₂ from first principles

Hongming Weng,¹ Gang Xu,¹ Haijun Zhang,² Shou-Cheng Zhang,^{2,3} Xi Dai,^{1,*} and Zhong Fang^{1,†}

¹*Beijing National Laboratory for Condensed Matter Physics and Institute of Physics, Chinese Academy of Sciences, Beijing 100190, China*

²*Department of Physics, McCullough Building, Stanford University, Stanford, California 94305-4045, USA*

³*Center for Advanced Study, Tsinghua University, Beijing 100084, China*

(Received 21 July 2011; published 30 August 2011)

Based on first-principles calculations, we predict a half-metallic surface state in layered bulk insulator NaCoO₂, with tunable surface hole concentration. The half-metallic surface has a single Fermi surface with a helical spin texture, similar to the surface state of topological insulators, but with the key difference of time-reversal symmetry breaking in the present case. We propose the realization of topological superconductivity and Majorana fermions when the half-metallic surface states are in proximity contact with a conventional superconductor.

DOI: [10.1103/PhysRevB.84.060408](https://doi.org/10.1103/PhysRevB.84.060408)

PACS number(s): 74.45.+c, 75.70.Tj, 73.20.-r

The possibility of realizing Majorana fermions in condensed matters as emergent excitations has stimulated great current interest. Majorana fermions are particles which are their own antiparticles.¹ They constitute only half of a usual fermion, and obey non-Abelian statistics,² which is the key ingredient for fault-tolerant topological quantum computation.³ The Majorana states associated with the zero energy mode have been predicted to exist in various systems,^{2,4–12} nevertheless, their experimental realizations remain challenging due to the requirements of extreme conditions such as a strong magnetic field, low temperature, or ultraclean samples. In this Rapid Communication, we will show that the NaCoO₂/superconductor heterostructure is a simple platform for realizing such states.

The simplest Majorana bound state is associated with a vortex core or edge in a two-dimensional (2D) topological $p_x + ip_y$ superconductor,^{5,6} which has a full pairing gap in the bulk but with gapless chiral edge states (which consists of Majorana fermions). Unfortunately, such topological superconductors are very rare in nature, and this leads to proposals of a possible “induced” $p_x + ip_y$ order parameter through the proximity effect, particularly for materials in contact with the simplest s -wave superconductors.^{7–12} The proposal by Fu and Kane⁷ is to use the surface state of topological insulators,^{13–15} where the spin degeneracy is removed, and yet strong proximity effect can be expected due to the characteristic helical spin texture of the Dirac-type surface state. The experimental setting, in principle, can be obtained from the laboratory, however, since most known three-dimensional topological insulators^{15–18} up to now are not good bulk insulators and important surface states may overlap with the bulk states, experiments have to wait for the development of well-controlled clean samples. It was proposed recently that semiconductor quantum wells with Rashba-type spin-orbit couplings (SOCs) in proximity to the s -wave superconductor will produce a similar effect.^{8–11} This may lower the experimental threshold, since well-controlled samples are available nowadays. Both proposals are encouraging, while experimental obstacles still remain. First, and most importantly, magnetic insulating layers or strong external magnetic field are required to break the time-reversal symmetry, which is not easy to implement experimentally; second, the Fermi surfaces in both cases are too small, and fine

control of the chemical potential is difficult for semiconductors in contact with a superconductor.

To avoid the complication required by breaking time-reversal symmetry (such as the use of magnetic insulating layers or a magnetic field), the most natural way is to start from a magnetic compound, rather than nonmagnetic topological insulators or semiconductor quantum wells. On the other hand, however, the following ingredients have to be satisfied over a wide energy or doping regime, in order to induce the $p_x + ip_y$ superconductivity through the proximity effect: (1) a two-dimensional metal with a single (or an odd number of) Fermi surface(s); and (2) a strong enough helical spin texture arising from SOC. Those conditions suggest that 2D single band half-metal materials with strong enough SOC's will be the best candidates.^{12,19} Following this strategy, we propose in this Rapid Communication that NaCoO₂ is such a unique compound which satisfies all those conditions simultaneously.

Bulk Na_xCoO₂ is a well-known layered compound crystallizing in a planar triangle lattice with the Co atom coordinated octahedrally by oxygen (Fig. 1). The Na atoms are interpolated between the CoO₂ layers, and its concentration x can be systematically tuned, resulting in a complex magnetic and electronic phase diagram.²⁰ In particular, the unconventional superconductivity at approximately $x = 0.35$,²¹ and the layered antiferromagnetic (AF) phase at approximately $x > 0.65$,^{22–24} have drawn much attention. For our purpose, however, we consider the stoichiometric NaCoO₂ (i.e., $x = 1.0$) and its surface state.

A NaCoO₂ single crystal (with $R\bar{3}m$ symmetry) is experimentally available,²⁵ and it is a simple band insulator with a band gap of more than 1.0 eV.²⁵ Its bulk insulating behavior has been indicated by transport²⁶ and NMR²⁷ measurements. Electronically, the Co-3d states split into t_{2g} and e_g manifolds under an oxygen octahedron crystal field, and all t_{2g} states are fully occupied (by six electrons) in the case without Na deficiency (corresponding to the nominal Co³⁺ case), resulting in a band gap between t_{2g} and e_g .^{25,27} The layered crystal structure guarantees that samples can be easily cleaved (Fig. 1), and two kinds of terminations, with or without a topmost Na layer, may be realized. Nevertheless, since the topmost Na¹⁺ ions are highly mobile, its concentration can be tuned depending on the experimental conditions,

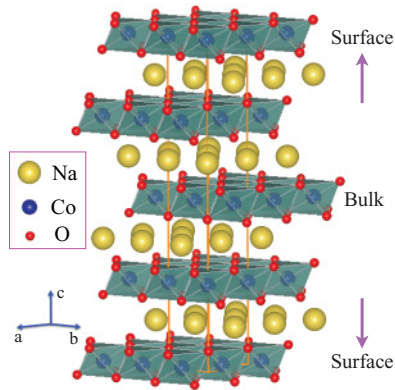


FIG. 1. (Color online) The structure of the NaCoO_2 slab consisting of five unit layers. After structure optimization, the surface Co-O bond lengths are slightly modified (by 0.07 \AA).

resulting in surface hole doping (indicated as y) but without significantly modifying the surface structure (the CoO_2 layer). In the extreme case, if all of the topmost Na is absent, a 0.5 hole will be introduced (i.e., $y = 0.5$). We study the (001) surface of NaCoO_2 by using first-principles calculations based on the plane-wave ultrasoft pseudopotential method, and the generalized gradient approximation (GGA) for the exchange-correlation functional. A slab consisting of five NaCoO_2 unit layer thickness (Fig. 1) and a 20-\AA vacuum region is used for the surface study, and the SOC is included from the fully relativistic pseudopotential. The cutoff energy for wave-function expansion is 30 Ry, and we use a 12×12 k -point mesh for the Brillouin zone sampling. The calculations are well converged with respect to the above settings. The calculations are further supplemented by the local density approximation (LDA) + Gutzwiller method,²⁸ in which the density functional theory is combined with the Gutzwiller variational approach such that the orbital fluctuation and kinetic renormalization coming from the correlation are all self-consistently treated.

By optimizing the surface (slab) structure without topmost Na layer, our calculations confirm that the surface CoO_2 layer remains well defined with only a slight ($\sim 0.07 \text{ \AA}$) modification of surface Co-O bond length (see Fig. 1). Another key result obtained from this calculation is that the hole only goes into the surface CoO_2 layer, while keeping all other CoO_2 layers inside the bulk to be insulating. There is only one band across the Fermi level (Fig. 2) which comes from one of the t_{2g} states of the topmost Co sites, while all other Co- t_{2g} states inside the bulk are fully occupied. It is therefore effectively a system with an insulating bulk but metallic surface, similar to topological insulators.^{13–15} The key difference lies in the fact that the surface state considered in this Rapid Communication breaks the time-reversal symmetry, in contrast to the case of topological insulators. In reality, the surface hole doping can be tuned by modifying the surface Na concentration, by interface charge transfer, or simply by gating. In the case of the proximity effect with a superconductor, such surface doping can naturally arise since many s -wave superconductors, such as Al, Pb, or Nb, are simple metals. In such a case, the insulating NaCoO_2 bulk can even simultaneously serve as a

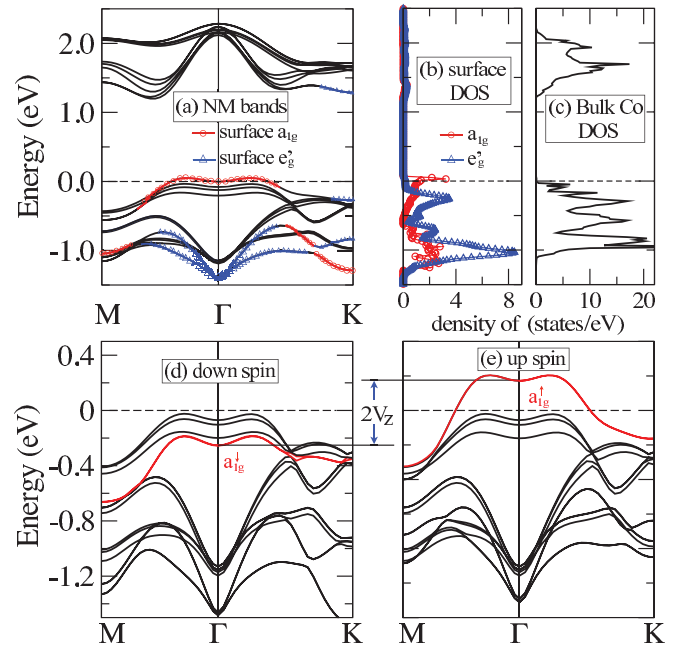


FIG. 2. (Color online) The calculated band structure and density of states (DOS) for a NaCoO_2 slab with surface hole concentration of $y = 0.3$. (a) The band structure of the nonmagnetic (NM) state. The projections to the a_{1g} and e'_g states of surface Co are indicated as red circles and blue triangles, respectively. (b) and (c) The corresponding DOS for the surface and bulk Co sites, respectively. The character of the insulating bulk with a metallic surface is seen. (d) and (e). The spin-resolved band structure of the ferromagnetic state with the V_z defined as the exchange splitting of the surface a_{1g} state.

substrate. In the following discussion, we will therefore neglect the topmost Na atoms and use the virtual crystal approximation to simulate the surface doping effect.

Figure 3 shows the magnetic properties of the NaCoO_2 surface as function of hole concentration y . The spin polarization is energetically favored for all hole concentrations ($0.5 > y > 0$), in close analogy to the layered AF phase of the Na_xCoO_2 bulk ($x \sim 0.75$),^{20,22,29} where each CoO_2 layer (with ~ 0.25 hole) orders ferromagnetically and the in-plane ferromagnetism contributes mostly to the energy gain with relatively weak interlayer AF coupling. The stabilization of ferromagnetism at the NaCoO_2 surface can be intuitively understood from Stoner instability [also similar to the discussion addressed for the layered AF bulk $\text{Na}_{0.75}\text{CoO}_2$ (Ref. 29)]. Due to the elongation of oxygen octahedra around the Co sites along the c axis, the Co- t_{2g} states will further split into a_{1g} and e'_g manifolds, with a_{1g} higher in energy. The a_{1g} state has mostly $3d_{3z^2-r^2}$ orbital character (with z defined along c), whose in-plane dispersion is relatively weak and “M” shaped, as observed in angle-resolved photoemission spectroscopy (ARPES) experiments.³⁰ As shown in Fig. 2(a), the wide region of the nearly flat bands around the valence-band maximum will produce a sharp DOS peak near the Fermi level [see Fig. 2(b)], which leads to the Stoner instability, and favors the ferromagnetic (FM) ground state for the surface. This mechanism is further supported by the electronic structure of the FM solution [Figs. 2(c) and 2(d)], where only the a_{1g} state is strongly spin polarized and the polarization of e'_g states

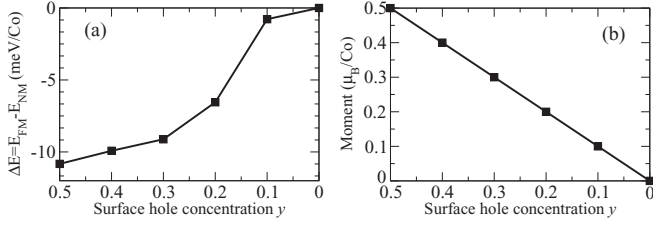


FIG. 3. The calculated magnetic properties of the NaCoO₂ surface as function of surface hole concentration y . (a) The stabilization energy of the ferromagnetic (FM) state with respect to the nonmagnetic (NM) state. (b) The magnetic moment of the surface CoO₂ layer.

is small. In the FM state, the spin polarization is strong enough to make the topmost CoO₂ layer a half-metal, as shown in Figs. 2 and 3, where the calculated magnetic moment exactly equals the number of holes. There is only one spin channel of the a_{1g} state that crosses the Fermi level, resulting in a half-metallic surface state with a single sheet of the Fermi surface.

We have to be aware of the effect of electron correlation beyond the GGA for the exchange-correlation potential. The LDA + Gutzwiller method²⁸ has been shown to be a powerful tool to take into account the correlation effect, and reproduce correctly the magnetic phase diagram of bulk Na_{*x*}CoO₂.²⁹ We have supplemented the LDA + Gutzwiller calculations for the surface, and find that the surface ferromagnetism is further stabilized (by ~ 8 meV/surface Co for $y = 0.3$). In fact, in the study for the bulk Na_{*x*}CoO₂ ($x > 0.6$), both GGA and LDA + Gutzwiller give qualitatively the same result, which compare well to experiments.²⁹ The AF state of bulk Na_{*x*}CoO₂ was observed for $x > 0.65$ with a maximum $T_c \sim 25$ K for $x \sim 0.8$, the layered ordering with spin orientation perpendicular to the plane was confirmed by neutron experiments,^{23,24} and its half-metallicity of the in-plane electronic structure is also supported by the ARPES measurements.^{31,32} Considering the layered nature and the similarity between the bulk AF phase and the surface, we conclude that a single-band half-metal can be realized at the NaCoO₂ surface with tunable hole concentration.

Turning on the SOC, the up and down spin bands will couple, while the characteristic single sheet of the Fermi surface still remains. In the presence of a surface, the asymmetrical surface potential will produce the Rashba-type SOC (which is automatically included in first-principles calculations). It turns out that the Rashba-type SOC plays important roles, resulting in the in-plane spin component, which has a helical spin texture for the states at the Fermi level (see Fig. 4). The in-plane component is actually rather strong, and contributes to more than 10% of the total moment from our first-principles calculations. Considering the single a_{1g} state of the NaCoO₂ surface and the threefold rotation symmetry, an effective surface Hamiltonian can be constructed as

$$H_0 = \sum_{\mathbf{k}} [\xi(\mathbf{k}) + V_z \sigma_z + \alpha(k_y \sigma_x - k_x \sigma_y)], \quad (1)$$

where $\xi(\mathbf{k}) = Ak_+k_- + B(k_+^6 + k_-^6) + C(k_+^3k_-^3)$ (with $k_{\pm} = k_x \pm ik_y$) gives the non-spin-polarized band structure, $V_z \sigma_z$ is the exchange splitting, and the last term is the Rashba-type

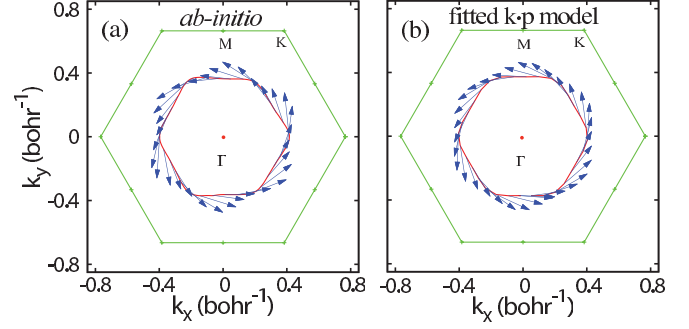


FIG. 4. (Color online) The Fermi surface and the helical spin texture of the NaCoO₂ surface (for $y = 0.3$) obtained from (a) first-principles calculations and (b) evaluation of the effective $k \cdot p$ model [Eq. (1), see the text] with parameter $A = 0.28$ eV \AA^2 , $B = 0.53$ eV \AA^6 , $C = -2.4$ eV \AA^6 , $\alpha = -0.066$ eV \AA , and $V_z = 0.22$ eV. The in-plane components of the spin are indicated as arrowed lines, while the perpendicular component (pointing to out of plane) is not shown.

SOC due to the surface. Evaluating the eigenvalues $\epsilon(\mathbf{k}) = \xi(\mathbf{k}) \pm \sqrt{V_z^2 + \alpha^2 k^2}$ with the parameters given in the caption of Fig. 4, the Fermi surface and its helical spin texture can be well reproduced [Fig. 4(b)]. Please note the hole-type carrier and the negative sign of the Rashba coupling α in our present case.

When the NaCoO₂ surface comes into contact with an s -wave superconductor, a pairing term $H_{\Delta} = \sum_{\mathbf{k}} [\Delta c_{\mathbf{k}\uparrow}^{\dagger} c_{\mathbf{k}\downarrow}^{\dagger} + \text{H.c.}]$ will be generated by the proximity effect, and the full Hamiltonian reads $H = H_0 + H_{\Delta}$, which has been carefully studied previously.^{8-11,19} The dominant pairing channel should have a spin-polarized $p_x + ip_y$ symmetry, whose order parameter is given as $\Delta_p^+(\mathbf{k}) = \frac{-\alpha k}{\sqrt{(V_z^2 + \alpha^2 k^2)}} \frac{k_y + ik_x}{k} \Delta$. In the limit of large V_z , following Ref. 9, the superconducting gap can be estimated as

$$E_g = \sqrt{\frac{2m^* \alpha^2}{V_z}} \left(1 + \frac{\mu}{V_z}\right) \Delta \approx 0.22 \Delta, \quad (2)$$

which is sizable. Here we use the following parameters: effective mass $m^* = 5m_0$, $\alpha = -0.066$ eV \AA , and $V_z = 0.22$ eV, obtained from our first-principles calculations. The size of Δ is determined by the superconducting gap of the

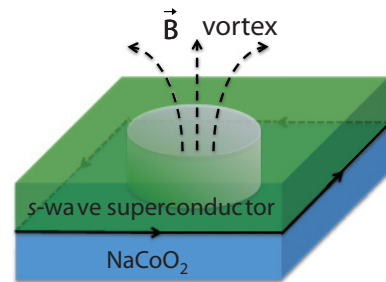


FIG. 5. (Color online) The schematic picture for the NaCoO₂/ s -wave superconductor heterostructure where the Majorana bound state is associated with the vortex core. The chiral Majorana edge state is also expected at the edge of interface.

s-wave superconductor and its interface coupling (hopping) with the NaCoO₂ side.

Once the $p_x + ip_y$ superconductivity is realized through the proximity effect, the Majorana bound states associated with the vortex core will be expected.^{7,8,19} The schematic experimental setting for the detection of Majorana fermions is shown in Fig. 5, where the absence of a magnetic insulating layer and/or magnetic field is the essential difference as compared to earlier proposals.⁷⁻⁹ In addition, due to the broken time-reversal symmetry (different from Fu and Kane's proposal⁷), a chiral Majorana edge state should exist at the interface (Fig. 5). Since the single-band half-metallic character of the NaCoO₂ surface can be realized in a large energy window (of ~ 0.2 eV), fine tuning of the chemical potential is not necessary. The large Fermi-surface size and the high carrier density should be also helpful for a sizable proximity effect, against the possible localization due to disorders. Among several possible choices

for the superconductor, it is particularly interesting to consider the Na_{*x*}CoO₂ superconductor with *x* at ~ 0.35 ,^{20,21} since the lattice structures are well matched. The NaCoO₂/*s*-wave superconductor heterostructure, therefore, provide a simple platform for realizing topological superconductivity and Majorana fermion bound states. This work can be generalized in several directions. Similar predictions can be also made for an AF Na_{*x*}CoO₂ (*x* > 0.65) thin film with an odd number of layers (which contribute to an odd number of Fermi surfaces), or for LiCoO₂, which has the same crystal and electronic structure as NaCoO₂.³³

We acknowledge the support from NSF of China and from the 973 program of China (Nos. 2007CB925000 and Nos. 2010CB923000), the US NSF under Grant No. DMR-0904264, and the Keck Foundation.

*daix@aphy.iphy.ac.cn

†zfang@aphy.iphy.ac.cn

¹See, for example, F. Wilczek, *Nat. Phys.* **5**, 614 (2009), and references therein.

²C. Nayak, S. H. Simon, A. Stern, M. Freedman, and S. Das Sarma, *Rev. Mod. Phys.* **80**, 1083 (2008).

³A. Kitaev, *Ann. Phys. (NY)* **303**, 2 (2003).

⁴M. Greiter, X. G. Wen, and F. Wilczek, *Nucl. Phys. B* **374**, 567 (1992).

⁵N. Read and D. Green, *Phys. Rev. B* **61**, 10267 (2000).

⁶S. Das Sarma, C. Nayak, and S. Tewari, *Phys. Rev. B* **73**, 220502(R) (2006).

⁷L. Fu and C. L. Kane, *Phys. Rev. Lett.* **100**, 096407 (2008).

⁸J. D. Sau, R. M. Lutchyn, S. Tewari, and S. Das Sarma, *Phys. Rev. Lett.* **104**, 040502 (2010).

⁹J. Alicea, *Phys. Rev. B* **81**, 125318 (2010).

¹⁰P. A. Lee, e-print arXiv:0907.2681.

¹¹A. C. Potter and P. A. Lee, *Phys. Rev. B* **83**, 094525 (2011).

¹²M. Duckheim and P. W. Brouwer, *Phys. Rev. B* **83**, 054513 (2011).

¹³C. L. Kane and E. J. Mele, *Phys. Rev. Lett.* **95**, 146802 (2005).

¹⁴B. A. Bernevig, and S. C. Zhang, *Phys. Rev. Lett.* **96**, 106802 (2006).

¹⁵H. J. Zhang, C.-X. Liu, X.-L. Qi, X. Dai, Z. Fang, and S.-C. Zhang, *Nat. Phys.* **5**, 438 (2009).

¹⁶D. Hsieh, D. Qian, L. Wray, Y. Xia, Y. S. Hor, R. J. Cava, and M. Z. Hasan, *Nature (London)* **452**, 970 (2008).

¹⁷Y. Xia, D. Qian, D. Hsieh, L. Wray, A. Pal, H. Lin, A. Bansil, D. Grauer, Y. S. Hor, R. J. Cava, and M. Z. Hasan, *Nat. Phys.* **5**, 398 (2009).

¹⁸Y. L. Chen, J. G. Analytis, J.-H. Chu, Z. K. Liu, S.-K. Mo, X.-L. Qi, H.-J. Zhang, D.-H. Lu, X. Dai, Z. Fang, S.-C. Zhang, I.-R. Fisher, Z. Hussain, and Z.-X. Shen, *Science* **325**, 178 (2009).

¹⁹S. B. Chung, H.-J. Zhang, X.-L. Qi, and S.-C. Zhang, e-print arXiv:1011.6422.

²⁰M. L. Foo, Y. Wang, S. Watauchi, H. W. Zandbergen, T. He, R. J. Cava, and N. P. Ong, *Phys. Rev. Lett.* **92**, 247001 (2004).

²¹K. Takada and H. Sakurai, H. Sakurai, E. Takayama-Muromachi, F. Izumi, R. A. Dilanian, and T. Sasaki, *Nature (London)* **422**, 53 (2003).

²²J. Sugiyama, J. H. Brewer, E. J. Ansaldo, H. Itahara, T. Tani, M. Mikami, Y. Mori, T. Sasaki, S. Hebert, and A. Maignan, *Phys. Rev. Lett.* **92**, 017602 (2004).

²³S. P. Bayrakci, I. Mirebeau, P. Bourges, Y. Sidis, M. Enderle, J. Mesot, D. P. Chen, C. T. Lin, and B. Keimer, *Phys. Rev. Lett.* **94**, 157205 (2005).

²⁴L. M. Helme, A. T. Boothroyd, R. Coldea, D. Prabhakaran, D. A. Tennant, A. Hiess, and J. Kulda, *Phys. Rev. Lett.* **94**, 157206 (2005).

²⁵Y. Takahashi, Y. Gotoh, and J. Akimoto, *J. Solid State Chem.* **172**, 22 (2003).

²⁶S. Kikkawa, S. Miyazaki, and M. Koizumi, *J. Solid State Chem.* **62**, 35 (1986).

²⁷C. de Vaulx, M. H. Julien, C. Berthier, M. Horvatic, P. Bordet, V. Simonet, D. P. Chen, and C. T. Lin, *Phys. Rev. Lett.* **95**, 186405 (2005).

²⁸X. Y. Deng, X. Dai, and Z. Fang, *Europhys. Lett.* **83**, 37008 (2008).

²⁹G. T. Wang, X. Dai, and Z. Fang, *Phys. Rev. Lett.* **101**, 066403 (2008).

³⁰T. Arakane, T. Sato, T. Takahashi, T. Fujii, and A. Asamitsu, *New J. Phys.* **13**, 043021 (2011).

³¹J. Geck, S. V. Borisenko, H. Berger, H. Eschrig, J. Fink, M. Knupfer, K. Koepnick, A. Koitzsch, A. A. Kordyuk, V. B. Zabolotnyy, and B. Büchner, *Phys. Rev. Lett.* **99**, 046403 (2007).

³²M. Z. Hasan, Y.-D. Chuang, D. Qian, Y. W. Li, Y. Kong, A. Kuprin, A. V. Fedorov, R. Kimmerling, E. Rotenberg, K. Rossnagel, Z. Hussain, H. Koh, N. S. Rogado, M. L. Foo, and R. J. Cava, *Phys. Rev. Lett.* **92**, 246402 (2004).

³³Y. Takahashi, Y. Totoh, J. Akimoto, S. Mizuta, K. Tokiwa, and T. Watanabe, *J. Solid State Chem.* **164**, 1 (2002).